Letter

Testing quantum foundations with quantum computers

Simanraj Sadana,[1] Lorenzo Maccone,[2] and Urbasi Sinha[1,*]

[1]*Light and Matter Physics, Raman Research Institute, Bengaluru-560080, India*

[2]*Dipartimento di Fisica and INFN Sezione di Pavia, University of Pavia, via Bassi 6, I-27100 Pavia, Italy*

(Received 28 November 2021; accepted 23 February 2022; published 1 April 2022)

We present two complementary viewpoints for combining quantum computers and the foundations of quantum mechanics. On the one hand, ideal devices can be used as test beds for experimental tests of the foundations of quantum mechanics: We provide algorithms for the Peres test for complex numbers in quantum superpositions and the Sorkin test of Born's rule. On the other hand, noisy intermediate-scale quantum devices can be benchmarked using these same tests. These are deep quantum benchmarks based on the foundations of quantum theory itself. We present test data from Rigetti hardware.

DOI: 10.1103/PhysRevResearch.4.L022001

Physics is experimental, so the postulates of all physical theories are based on experiments. Here, we propose to use quantum computers for direct experimental tests of two of the postulates of quantum mechanics. In the ideal case, assuming perfect hardware, they are especially suited to this aim as they are quantum systems with a large number of degrees of freedom. In contrast, in the nonideal case of noisy intermediate-scale quantum (NISQ) devices, one can assume that quantum mechanics is valid and use these tests for benchmarking [1–3] the device at a deep quantum level, since they are based on the very foundations (the postulates) of the theory. In other words, assuming perfect hardware, one can test quantum mechanics; assuming quantum mechanics, one can test the hardware. Relaxing both assumptions, one can perform self-consistency checks to test both.

We present two such experimental tests: We give algorithms and quantum machine code for the Peres and the Sorkin tests and run them on Rigetti quantum computers. The first one is a test of the state postulate of quantum mechanics (i.e., the superposition principle), which claims that quantum states live in a *complex* Hilbert space. In principle, one could imagine a quantum mechanics based on real [4,5], complex, or quaternionic Hilbert spaces [6]: The choice is based on the outcome of experiments, such as the Peres one; see also Refs. [7–12]. The fact that complex numbers are necessary (and sufficient) has interesting implications, e.g., it implies that quantum states are locally discriminable [13] and it is connected to the locality of some quantum phenomena [7]. The second experimental test, proposed by Sorkin [14], is a test of the Born postulate. Born's rule declares that quantum probability is the square modulus of a scalar product in the state space. A failure (or an extension [15]) of Born's rule would result in a new physical effect: the presence of genuinely n-fold superpositions that cannot be reduced to an iteration of the usual twofold superpositions that we find in textbook quantum mechanics [15–17]. Thanks to our implementation, we also ran both tests at the same time for a class of states. In contrast to previous tests [8,9,18–20], ours do not use custom-built setups; they permit arbitrary initial states and can be easily scaled up as new reliable quantum computers become available. Our assumptions are that the quantum state is a vector in a Hilbert space (superposition principle) without specifying whether the Hilbert space is defined on a real, complex, or quaternion field, that the evolution is described by unitary transformations (i.e., the Schrödinger equation), and that the probabilities of measurement outcomes are functions of the scalar product of the state and some basis vectors. The last assumption is only a part of the Born's rule postulate, which states that the probabilities are equal to the square moduli of the scalar product. The Sorkin test is independent of whether the required field is real, complex, or quaternionic, so it is independent of the results of the Peres test. In the case of the Peres test, we are additionally assuming Born's rule (verified by the Sorkin test). Regarding the dependence of the Peres test on the Sorkin test, we note that we can assume the validity of Born's rule in the Peres test because we are testing the former separately using the Sorkin test (which is independent of the Peres test) and then we also perform both tests jointly.

There are multiple advantages of doing these (and other) fundamental tests on quantum computers: (i) Both tests are performed on the same hardware, which prevents possible biases that may arise from a tailored experimental setup. At the same time, it is simple to translate the proposed algorithms to different quantum computer architectures, if one wants to confirm the results independently. (ii) It is possible to perform both experiments *at the same time* (see below), which is important since, as discussed below, the two experiments are not entirely independent of each other. (iii) These experiments are easily scalable to large dimensions, once reliable quantum computers are available. (iv) As discussed, one can reverse

*usinha@rri.res.in

perspective: Under the assumption that quantum mechanics is correct, these tests become deep benchmarks for a quantum computer.

We initially believed that we could translate the Peres and Sorkin tests into quantum algorithms in a straightforward manner, but we found that we had to modify these tests in a nontrivial way both due to the practical limitations of current NISQ devices and due to the fundamental limitations of the gate model of quantum computation, which would require, as an input to an unmodified Peres algorithm, the same quantity γ (defined below) that one then measures.

Peres test. The state postulate claims the following: "The pure state of a system is described by a normalized vector $|\psi\rangle$ in a complex Hilbert space." Like all physical postulates, it is based on experimental data, and the Peres test specifically refers to whether one needs complex numbers, real numbers [5], quaternions [6,16,21], octonions [17,22], etc.; however, it does not question the Hilbert space structure of the theory. For example, we accept the natural assumption that the Hilbert space dimension is equal to the system's number of degrees of freedom, namely, of independent outcomes of a nondegenerate observable (dropping this assumption [4,5], one needs different tests for the complexity of quantum mechanics [7–9,11], based on the locality of measurement outcomes). Octonions can be discarded upon observing that they are not associative for multiplication (interestingly, this means that different combinations of twofold interferences may give different results, which would give the same signature as a failure of the Sorkin test).

We now review the Peres test [6]. Consider two pure states $|\psi_1\rangle$ and $|\psi_2\rangle$ and their superposition $|\psi_{12}\rangle = \alpha\,|\psi_1\rangle + \beta\,|\psi_2\rangle$, with α, β being nonzero real numbers (in case of complex α and β, their phases can be absorbed as the phases of $|\psi_1\rangle$ and $|\psi_2\rangle$ respectively). If we project it on, say, $|1\rangle$ (any other state would give similar results), then, assuming complex Hilbert spaces, the probability of successful projection is

$$|\langle 1|\psi_{12}\rangle|^2 = |\alpha\,\langle 1|\psi_1\rangle|^2 + |\beta\,\langle 1|\psi_2\rangle|^2 + 2\alpha\beta|\langle 1|\psi_1\rangle\,\langle 1|\psi_2\rangle|\cos\varphi_{12} \quad (1)$$

$$\Rightarrow \cos\varphi_{12} = \frac{|\langle 1|\psi_{12}\rangle|^2 - |\alpha\,\langle 1|\psi_1\rangle|^2 - |\beta\,\langle 1|\psi_2\rangle|^2}{2\alpha\beta|\langle 1|\psi_1\rangle\,\langle 1|\psi_2\rangle|}, \quad (2)$$

with $\varphi_{12} = \arg(\langle 1|\psi_1\rangle\,\langle\psi_2|1\rangle)$. If instead we assume that real Hilbert spaces are sufficient, the term $\cos\varphi_{12}$ can only take the values ± 1. We can rewrite the left-hand side of (2) in terms of experimental values as

$$\gamma_{12} := \frac{p_{12} - \alpha^2 p_1 - \beta^2 p_2}{2\alpha\beta\sqrt{p_1 p_2}}, \quad (3)$$

with p_{12}, p_1, and p_2 being the experimental probabilities of projection onto $|1\rangle$ of $|\psi_{12}\rangle$, $|\psi_1\rangle$, and $|\psi_2\rangle$. If we experimentally find that $\gamma_{12} = \pm 1$ *always*, then a real quantum theory is sufficient. If we find states for which $|\gamma_{12}| < 1$, then it is necessary to use a complex or quaternionic quantum theory. If $|\gamma| > 1$, the superposition principle is violated.

To discriminate between a complex and a quaternionic theory, we need a further step, based on the identity

$$\cos^2 a + \cos^2 b + \cos^2 c - 2\cos a\cos b\cos c = 1, \quad (4)$$

valid for any a, b, c real numbers with $a + b + c = 0$. Consider three pure states $|\psi_1\rangle, |\psi_2\rangle, |\psi_3\rangle$, and take superpositions of two at a time. We will have three quantities of the type given in (2) with φ_{12}, φ_{23}, or φ_{31}, one for each pair. Since $\varphi_{12} + \varphi_{23} + \varphi_{31} = 0$, the identity (4) holds for these three angles *if* a complex quantum theory is sufficient. Otherwise, if a quaternionic theory is necessary, the amplitudes cannot be represented by vectors in a two-dimensional (2D) plane, and therefore the left-hand side of (4) is less than 1 in general. One can detect this by analyzing the quantity $F = \gamma_{12}^2 + \gamma_{23}^2 + \gamma_{31}^2 - 2\gamma_{12}\gamma_{23}\gamma_{31}$ (where γ_{23}, γ_{31} are defined similarly to γ_{12}, but using the state $|\psi_3\rangle$). If the experimentally measured F is *always* 1 for all states, then a complex theory is sufficient (no quaternions, octonions, etc., are needed) since all the γ's can be written as cosines, and (4) holds. Otherwise, if $|F| < 1$, then we must employ quarternions. Finally, if $|F| > 1$, the superposition principle is violated, as the states cannot be represented as vectors.

The above Peres proposal can be directly implemented on a quantum computer using a unary encoding (one qubit per system) where orthogonal states are mapped into separate physical qubits and their superpositions are obtained through interferences among them, but our tests showed that such a procedure is highly sensitive to noise and will be reported elsewhere [23]. Moreover, one has to make sure that the algorithm does not contain as input the quantity $\cos\varphi_{12}$ of (2), which would render the whole procedure circular. We now present a nontrivial way to overcome both problems: It is suited to current NISQ devices, and the cosine term only arises from quantum interference of different paths.

The trick is to prepare a two-qubit factorized state $|\psi_1\rangle\,|\psi_2\rangle$ with $|\psi_k\rangle = a_k\,|0\rangle + e^{i\varphi_k} b_k\,|1\rangle$ ($a_k \in [0, 1]$, $b_k = \sqrt{1 - a_k^2}$) and then project it onto the anticorrelated subspace spanned by $|01\rangle$ and $|10\rangle$. This produces a state proportional to

$$a_1 b_2 e^{i\varphi_2}\,|01\rangle + a_2 b_1 e^{i\varphi_1}\,|10\rangle \propto a_1 b_2 e^{i\varphi_2}(\alpha^*\,|\Psi^+\rangle \quad (5)$$

$$+ \beta\,|\Psi^-\rangle) + a_2 b_1 e^{i\varphi_1}(\beta^*\,|\Psi^+\rangle - \alpha\,|\Psi^-\rangle), \quad (6)$$

with $|\Psi^+\rangle = \alpha\,|01\rangle + \beta\,|10\rangle$, $\quad |\Psi^-\rangle = \beta^*\,|01\rangle - \alpha^*\,|10\rangle$.

By projecting this state onto $|\Psi^+\rangle$, we can see the interference among the two $|\Psi^+\rangle$ paths present in the state (6). Indeed,

$$|\langle\Psi^+|\psi_1\psi_2\rangle|^2 = |\alpha|^2|\langle 01|\psi_1\psi_2\rangle|^2 + |\beta|^2|\langle 10|\psi_1\psi_2\rangle|^2 + 2\mathrm{Re}\{\alpha^*\beta\}|\langle 01|\psi_1\psi_2\rangle\,\langle 10|\psi_1\psi_2\rangle|\cos\varphi_{12}$$
$$\Rightarrow \cos\varphi_{12} = \frac{|\langle\Psi^+|\psi_1\psi_2\rangle|^2 - |\alpha|^2|\langle 01|\psi_1\psi_2\rangle|^2 - |\beta|^2|\langle 10|\psi_1\psi_2\rangle|^2}{2\mathrm{Re}\{\alpha^*\beta\}|\langle 01|\psi_1\psi_2\rangle\,\langle 10|\psi_1\psi_2\rangle|}. \quad (7)$$

Projections onto an entangled state can be implemented by a CNOT gate and a single-qubit rotation followed by a measurement in the computational basis. The experimental values of the γ's can then be obtained by measuring the probability of projection of this state (and of the projection of $|\psi_1\psi_2\rangle$ onto $|01\rangle$ and $|10\rangle$). The algorithm to create and measure these states is given pictorially in Fig. 1. Once the γ's are measured, we can test, by hypothesis testing, whether their experimental values are compatible with ± 1, and similarly for

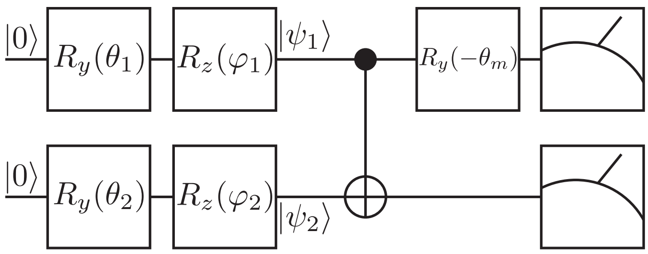

FIG. 1. Graphical depiction of the algorithm to calculate the γ factor of (7) by creating and projecting superpositions of arbitrary states. The states are created from unitary rotations $R_\ell(\lambda)$ of an angle λ around the ℓ axis, with $a_k = \cos\theta_k/2$, $b_k = \sin\theta_k/2$, followed by a CNOT gate and a rotation by angle $-\theta_m$ for desired projection. For example, to project on $\alpha\,|01\rangle + \beta\,|10\rangle$, choose $\theta_m = 2\cos^{-1}\alpha$ and record the counts of $|01\rangle$. The unentangled projections $|\langle 01|\psi_1\psi_2\rangle|^2$, etc., that are necessary for the γ's can be measured by a similar circuit where the CNOT gate and the single-qubit rotation at the end are removed.

F. In principle, the Peres test should check that $F = 1$ for *all* states, which is, of course, not feasible. However, by choosing sets of (uniform) random states, we sample the Hilbert space uniformly.

The experimental results are presented in Fig. 2. The fact that a complex quantum theory is necessary, and it is also sufficient as quaternions are not required, is confirmed by our results up to experimental error (which we fully characterized). All the circuits are run for 10^4 shots, and the limited sample gives rise to significant statistical fluctuations in the results, indicated in the plots by 3σ confidence intervals. We also plotted the values obtained from simulations on Rigetti's quantum virtual machine (QVM). Because of noises in the quantum computer, the result of the Peres test has statistically significant deviations from the theoretical values. However, when we take into account the dominant sources of systematic errors (readout and dephasing errors here) in the gates in a noisy simulation, we observe that the deviations in the results are accounted for. We choose the noise parameters for each type of noise from the device specifications provided by Rigetti. Including the specified errors reproduces the deviations in the value of F up to statistical fluctuation. This confirms that the observed value of $F < 1$ is due to the noises, and we cannot reject the hypothesis that complex numbers are sufficient. We explore the effects of different types of errors in Ref. [23].

Since the value of F is sensitive to the number and amount of errors present in the hardware, it can be used to benchmark the quantum computer if one assumes the correctness of quantum mechanics, e.g., in the presence of dephasing noise (parametrized by $0 \leqslant p \leqslant 1$). If we simulate the Peres test using an artificial dephasing noise model, we observe that the deviation of F from 1 towards zero increases with the increase in the amount of noise. Namely, by finding the amount of dephasing noise that reproduces the experimentally observed deviation of F, we can get a bound on the amount of dephasing noise in the system [23]. Similar bounds can be determined for other types of noises.

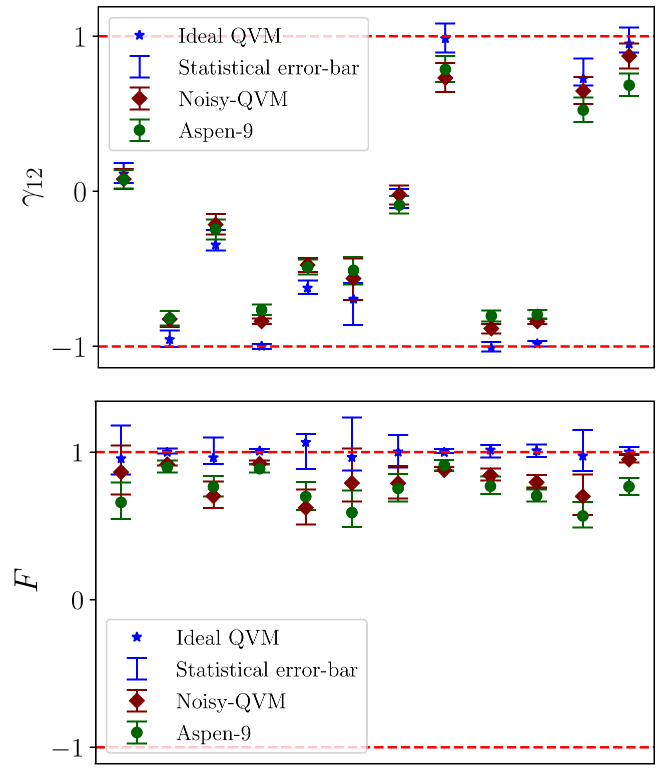

FIG. 2. Plots of the γ_{12} and of F for different sets of (uniformly distributed) random states. The green circles are the measured outputs on a Rigetti Aspen-9 device, the blue stars are the (ideal) quantum prediction from Rigetti's quantum virtual machine (QVM), and the red diamonds are the quantum prediction that takes into account the systematic noise sources (the noise parameters are obtained from Rigetti's own calibration data). Most γ values are different from ± 1, which implies that a real Hilbert space is insufficient. The values of F are all smaller than 1, but they are all statistically compatible with the value corrected by taking into account the readout and dephasing errors in the hardware (as explained in the main text). None of the values of F are outside the interval $[-1, 1]$, so the superposition principle is not violated.

Sorkin test. The measurement postulate (Born's rule) claims the following: "The probability that a measurement of a property O, described by the operator with spectral decomposition $\sum_j o_j\,|j\rangle\,\langle j|$, returns a value o_j, given that the system is in state $|\psi\rangle$, is $p(o_j|\psi) = |\langle\psi|j\rangle|^2 = |x_j|^2$, with $|\psi\rangle = \sum_j x_j\,|j\rangle$" [24].

The linearity of quantum mechanics implies that, if a value o_j of some system property is determined by two or more indistinguishable pathways, the probability of measuring such value is obtained from the sum (interference) of the amplitudes for each (superposition principle). This interference is encoded in the postulate by the scalar product $\langle\psi|j\rangle$ (whose definition contains a sum). The exponent 2 in the probability postulate implies that the superposition of more than two pathways gives the same probability that is obtained by separately considering the interference of all the *couples* of paths independently [14,15]. Namely, no *genuinely n-path* interference effects appear for $n > 2$. In fact, for $n = 3$, assuming Born's rule, consider the following probabilities:

$$p_{123} = \left|\left(\frac{\langle 1| + \langle 2| + \langle 3|}{\sqrt{3}}\right)|\psi\rangle\right|^2 = \frac{|x_1 + x_2 + x_3|^2}{3}, \quad (8)$$

$$p_{12} = \left|\left(\frac{\langle 1| + \langle 2|}{\sqrt{2}}\right)|\psi\rangle\right|^2 = \frac{|x_1 + x_2|^2}{2}, \text{ etc.}, \quad (9)$$

$$p_1 = |\langle 1|\psi\rangle|^2 = |x_1|^2, \text{ etc.}, \quad (10)$$

where the bras refer to the O eigenstates $|j\rangle$, the term (8) refers to a three-path interference, (9) refers to two-path interference, and (10) is the probability of each path by itself. The exponent 2 ensures that the multipath probability can always be expressed in terms of the two-path and single-path ones. Indeed the quantity

$$\kappa_3 = 3p_{123} - 2(p_{12} + p_{23} + p_{13}) + p_1 + p_2 + p_3 \quad (11)$$

is identically null thanks to the following identity, valid for any three complex numbers x_1, x_2, x_3:

$$3\left|\frac{x_1 + x_2 + x_3}{\sqrt{3}}\right|^2 - 2\left[\left|\frac{x_1 + x_2}{\sqrt{2}}\right|^2 + \left|\frac{x_1 + x_3}{\sqrt{2}}\right|^2 + \left|\frac{x_2 + x_3}{\sqrt{2}}\right|^2\right] + |x_1|^2 + |x_2|^2 + |x_3|^2 = 0. \quad (12)$$

Sorkin [14] proposed to check the form of Born's rule and the superposition principle by *measuring* the probabilities (8)–(10) and calculating the experimental value of κ_3 to check if it is null (up to statistical error). This can be extended to arbitrary n. In fact, if we assume (or measure experimentally) that the κ_j's up to $j = n - 1$ are null, one can show by induction that

$$\kappa_n = \left|\sum_{j=1}^{n} x_j\right|^2 - \sum_{j,k>j}^{n-1,n} |x_j + x_k|^2 + (n-2)\sum_{j=1}^{n} |x_j|^2, \quad (13)$$

so that one can incrementally increase n by just measuring the n-path, two-path, and one-path probabilities.

Importantly, one has to ensure that the pathways are distinguishable (i.e., they are described by orthogonal states); otherwise interferences are not obtained through simple sums as in (8)–(10). Initial experiments were carried out following Sorkin's proposal of multislit experiments [18] which are only approximately orthogonal (looping paths that go through multiple slits exist [25–27]). As we do here, some tests used orthogonal states [28], where a null result is easier to evaluate.

To implement a Sorkin test on a quantum computer, we need to create an arbitrary superposition of n orthogonal pathways. This can be done using n qubits with a unary encoding [23] or, more efficiently and in a less error-prone manner, with $\log_2 n$ qubits in a binary encoding. Start with $n = 3$: The circuit to create arbitrary three-level states with binary encoding is presented in Fig. 3(a). It implements the transformation $U(\theta_1, \varphi_1, \theta_2, \varphi_2)|00\rangle$, which prepares the state

$$|\psi\rangle = \cos\frac{\theta_1}{2}e^{-i\varphi_1/2}|00\rangle + \sin\frac{\theta_1}{2}e^{i\varphi_1/2}\cos\frac{\theta_2}{2}e^{-i\varphi_2/2}|10\rangle + \sin\frac{\theta_1}{2}e^{i\varphi_1/2}\sin\frac{\theta_2}{2}e^{i\varphi_2/2}|11\rangle, \quad (14)$$

where θ_k and φ_k are defined in the figure caption and are chosen randomly. To get the probabilities (8)–(10), we need to project $|\psi\rangle$ onto a state $\langle\psi'|$ such as $(\langle 00| + \langle 10| + \langle 11|)/\sqrt{3}$,

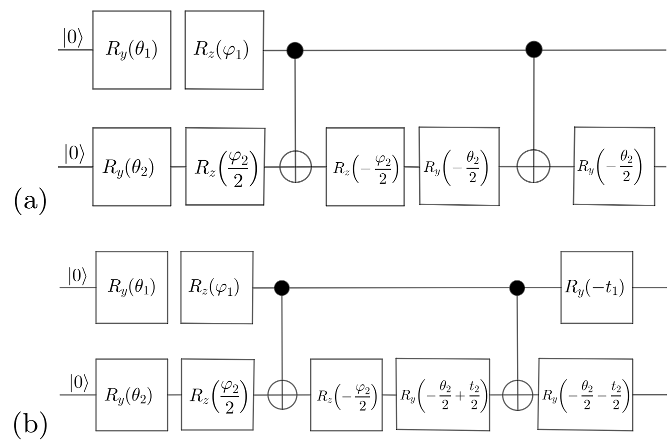

FIG. 3. Sorkin-test circuits. (a) Circuit to prepare arbitrary three-level states (14): $R_\ell(\lambda)$ represents a rotation around the ℓ axis by an angle λ. (b) Complete circuit that includes also the measurements. The parameters t_1 and t_2 are used to select the different measurements. For example, the projection onto $|00\rangle + |10\rangle + |11\rangle$ discussed in the text is obtained by choosing $t_1 = 2\cos^{-1}(1/\sqrt{3})$, $t_2 = 2\cos^{-1}(1/\sqrt{2})$.

etc. The state $\langle\psi'| = \langle 00|\,U^\dagger(t_1, f_1, t_2, f_2)$ is implemented by the adjoint of the circuit of Fig. 3(a) with appropriate t_1, f_1, t_2, f_2, and the projection is $\langle 00|U^\dagger(t_1, f_1, t_2, f_2)U(\theta_1, \varphi_1, \theta_2, \varphi_2)|00\rangle$. The simplified quantum circuit to implement $U^\dagger(t_1, 0, t_2, 0)U(\theta_1, \varphi_1, \theta_2, \varphi_2)$ is shown in Fig. 3(b). Measurements in the computational basis can be done by setting $t_1 = t_2 = 0$ and getting all the projections from the same run of the circuit. Using this circuit, we performed the three-level Sorkin test on a number of randomly chosen states. The results are presented in Fig. 4, and they confirm that κ_3 is statistically compatible with zero, as expected.

The extension to arbitrary n can be obtained from the measurement of the n-path probability: It can be implemented using a Hadamard gate on each path followed by computational basis measurement if n is a power of 2 or, in general, from a circuit whose adjoint creates a uniform superposition

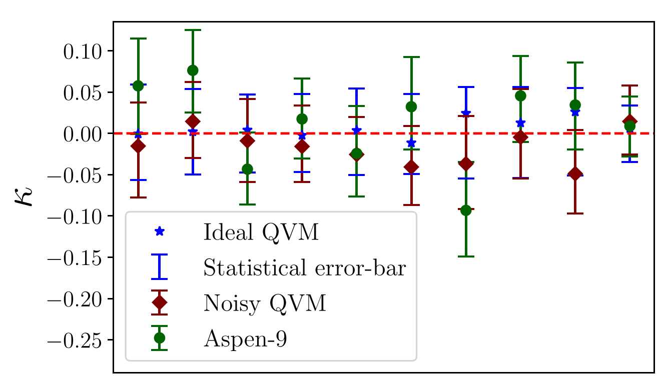

FIG. 4. Plot of κ_3 of Eq. (11) of the Sorkin test for randomly chosen states performed using the circuit of Fig. 3(b). All obtained values are compatible with the theoretical value $\kappa_3 = 0$ expected from standard quantum mechanics. The error bars are produced using the same method as in the case of the Peres test in Fig. 2.

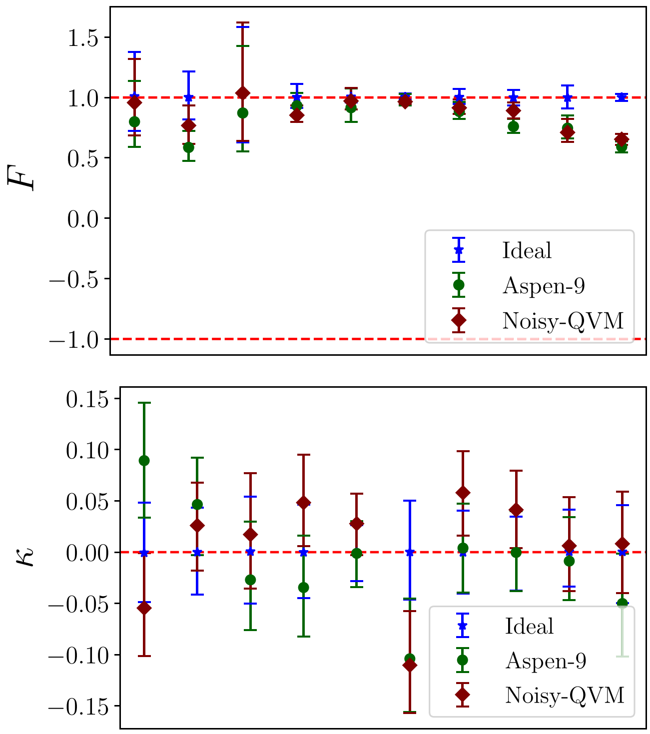

FIG. 5. Results of the joint Peres and Sorkin test using the same set of states and circuits for both. The data acquired to perform the Sorkin test in this case were sufficient to perform the Peres test, and therefore the same data set is used to plot both κ_3 and F. The results of the joint Peres-Sorkin test are consistent with theoretical expectations, taking into account the readout and dephasing errors present in the system. These results are also consistent with the results of the standalone versions of the Peres test and the Sorkin test shown in Figs. 2 and 4 (the values are, however, different because the set of random states used in each case is different).

starting from a $|0\cdots0\rangle$ state. The probability of obtaining all zeros from this measurement gives the first term of the hierarchy, namely, the first sum in (13), i.e., Eq. (8) for $n = 3$. Then we only require two-path and one-path probabilities that can be obtained with a trivial extension of the above procedure: Translate to binary and then use two-qubit correlations for the two-path probabilities or measure the computational basis for the one-path probabilities. This is sufficient, in principle, to incrementally scale the Sorkin test to large $n = 2^N$ using N qubits [23], although in practice, current NISQ device limitations prevent us from testing for large n as errors increase with increasing number of qubits.

Interestingly, our algorithmic procedure allows us to perform the Peres and Sorkin tests *jointly* for a class of states. Instead of using the above procedure to prepare the Sorkin-test state, we use the Peres-test circuit of Fig. 1 to produce and project a set of randomly generated states of the form $|\psi_1\psi_2\rangle = a\,|00\rangle + b\,|01\rangle + c\,|10\rangle + d\,|11\rangle$. We then consider the projections onto $|00\rangle + |01\rangle + |10\rangle$, onto the two path states $|00\rangle + |01\rangle$, $|00\rangle + |10\rangle$, and onto $|01\rangle + |10\rangle$ and for the singles. For the Sorkin test, we make an additional projection on $|00\rangle + |01\rangle + |10\rangle$ by replacing the CNOT gate and single qubit rotation at the end with the adjoint of the circuit that transforms $|00\rangle \to (|00\rangle + |01\rangle + |10\rangle)/\sqrt{3}$ and then measuring $|00\rangle$. Since the state $|11\rangle$ never appears in these measurements, this procedure is equivalent to first projecting the state $|\psi_1\psi_2\rangle$ onto the subspace spanned by $|00\rangle$, $|01\rangle$, and $|10\rangle$ and then performing the Sorkin test on the projected state (results are shown in Fig. 5).

The experimental results presented here refer to the output of algorithms we ran on an Aspen-9 machine provided by Rigetti Computing. The source code of our algorithms is written in PYTHON, using the PYQUIL library [29], the quantum instruction language developed for the Rigetti software development kit (SDK) [30].

Conclusions. We propose and implement quantum algorithms to test some of the physical principles behind two postulates of quantum mechanics: the complex nature of quantum Hilbert spaces and the form of Born's rule. We also perform both tests at the same time. We present results on a NISQ device. The source codes of our algorithms are available [31].

Acknowledgments. L.M. acknowledges funding from MIUR Dipartimenti di Eccellenza 2018-2022 Project No. F11I18000680001 and from the U.S. Department of Energy, Office of Science, National Quantum Information Science Research Centers, Superconducting Quantum Materials and Systems Center (SQMS). We acknowledge support from Rigetti, and, in particular, from Matt Reagor. U.S. acknowledges partial support provided by the Ministry of Electronics and Information Technology (MeitY), Government of India, under a grant for Centre for Excellence in Quantum Technologies with Ref. No. 4(7)/2020 - ITEA, QuEST-DST Project No. Q-97 of the Government of India, and the QuEST-ISRO research grant.

[1] K. Wright, K. M. Beck, S. Debnath, J. M. Amini, Y. Nam, N. Grzesiak, J.-S. Chen, N. C. Pisenti, M. Chmielewski, C. Collins, K. M. Hudek, J. Mizrahi, J. D. Wong-Campos, S. Allen, J. Apisdorf, P. Solomon, M. Williams, A. M. Ducore, A. Blinov, S. M. Kreikemeier *et al.*, Benchmarking an 11-qubit quantum computer, Nat. Commun. **10**, 5464 (2019).

[2] J. Eisert, D. Hangleiter, N. Walk, I. Roth, D. Markham, R. Parekh, U. Chabaud, and E. Kashefi, Quantum certification and benchmarking, Nat. Rev. Phys. **2**, 382 (2020).

[3] K. Georgopoulos, C. Emary, and P. Zuliani, Quantum computer benchmarking via quantum algorithms, arXiv:2112.09457.

[4] W. K. Wootters, Optimal information transfer and real-vector-space quantum theory, in *Quantum Theory: Informational Foundations and Foils*, edited by G. Chiribella and R. Spekkens, Fundamental Theories of Physics Vol. 181 (Springer, New York, 2016), pp. 21–43.

[5] E. C. G. Stueckelberg, Quantum theory in real Hilbert space, Helv. Phys. Acta **33**, 727 (1960).

[6] A. Peres, Proposed Test for Complex versus Quaternion Quantum Theory, Phys. Rev. Lett. **42**, 683 (1979).

[7] M.-O. Renou, D. Trillo, M. Weilenmann, T. P. Le, A. Tavakoli, N. Gisin, A. Acin, and M. Navascues, Quantum theory based on

real numbers can be experimentally falsified, Nature **600**, 625 (2021).

[8] L. M. Procopio, L. A. Rozema, Z. J. Wong, D. R. Hamel, K. O'Brien, X. Zhang, B. Dakic, and P. Walther, Single-photon test of hyper-complex quantum theories using a metamaterial, Nat. Commun. **8**, 15044 (2017).

[9] R. Keil, T. Kaufmann, T. Kauten, S. Gstir, C. Dittel, R. Heilmann, A. Szameit, and G. Weihs, Hybrid waveguide-bulk multi-path interferometer with switchable amplitude and phase, APL Photon. **1**, 081302 (2016).

[10] S. Gstir, E. Chan, T. Eichelkraut, A. Szameit, R. Keil, and G. Weihs, Towards probing for hypercomplex quantum mechanics in a waveguide interferometer, New J. Phys. **23**, 093038 (2021).

[11] M.-C. Chen, C. Wang, F.-M. Liu, J.-W. Wang, C. Ying, Z.-X. Shang, Y. Wu, M. Gong, H. Deng, F.-T. Liang, Q. Zhang, C.-Z. Peng, X. Zhu, A. Cabello, C.-Y. Lu, and J.-W. Pan, Ruling Out Real-Valued Standard Formalism of Quantum Theory, Phys. Rev. Lett. **128**, 040403 (2022).

[12] K.-D. Wu, T. Varun Kondra, S. Rana, C. M. Scandolo, G.-Y. Xiang, C.-F. Li, G.-C. Guo, and A. Streltsov, Operational Resource Theory of Imaginarity, Phys. Rev. Lett. **126**, 090401 (2021).

[13] G. Chiribella, G. M. D'Ariano, and P. Perinotti, Informational derivation of quantum theory, Phys. Rev. A **84**, 012311 (2011).

[14] R. D. Sorkin, Quantum mechanics as quantum measure theory, Mod. Phys. Lett. A **09**, 3119 (1994).

[15] B. Daki, T. Paterek, and C. Brukner, Density cubes and higher-order interference theories, New J. Phys. **16**, 023028 (2014).

[16] K. Zyczkowski, Quartic quantum theory: an extension of the standard quantum mechanics, J. Phys. A: Math. Theor. **41**, 355302 (2008).

[17] C. M. Lee and J. H. Selby, Higher-order interference in extensions of quantum theory, Found. Phys. **47**, 89 (2017).

[18] U. Sinha, C. Couteau, T. Jennewein, R. Laflamme, and G. Weihs, Ruling out multi-order interference in quantum mechanics, Science **329**, 418 (2010).

[19] D. K. Park, O. Moussa, and R. Laflamme, Three path interference using nuclear magnetic resonance: a test of the consistency of Born's rule, New J. Phys. **14**, 113025 (2012).

[20] H. Kaiser, E. A. George, and S. A. Werner, Neutron interferometric search for quaternions in quantum mechanics, Phys. Rev. A **29**, 2276(R) (1984).

[21] S. L. Adler, Generalized quantum dynamics, Nucl. Phys. B **415**, 195 (1994).

[22] S. De Leo and K. Abdel-Khalek, Octionionic quantum mechanics and complex geometry, Prog. Theor. Phys. **96**, 823 (1996).

[23] S. Sadana, L. Maccone, and U. Sinha, Quantum computational tests of the Born rule (unpublished).

[24] Using Naimark's theorem, this formulation encompasses also measurements described by positive operator-valued measures (POVMs). It can be extended trivially to nondegenerate observables by adding a degeneracy index: $O = \sum_{jk} o_j |j,k\rangle\langle j,k|$ gives a probability $p(o_j|\psi) = \sum_k |\langle\psi|j,k\rangle|^2$ [32].

[25] R. Sawant, J. Samuel, A. Sinha, S. Sinha, and U. Sinha, Nonclassical Paths in Quantum Interference Experiments, Phys. Rev. Lett. **113**, 120406 (2014).

[26] G. Rengaraj, U. Prathwiraj, S. N. Sahoo, R. Somashekhar, and U. Sinha, Measuring the deviation from the superposition principle in interference experiments, New J. Phys. **20**, 063049 (2018).

[27] A. Sinha, A. H. Vijay, and U. Sinha, On the superposition principle in interference experiments, Sci. Rep. **5**, 10304 (2015).

[28] I. Söllner, B. Gschösser, P. Mai, B. Pressl, Z. Vörös, and G. Weihs, Testing Born's rule in quantum mechanics for three mutually exclusive events, Found. Phys. **42**, 742 (2012).

[29] See, https://github.com/rigetti/pyquil/.

[30] Rigetti SDK at https://qcs.rigetti.com/sdk-downloads.

[31] See, http://www.rri.res.in/QuicLab/Peres_Sorkin/.

[32] G. Lüders, Über die Zustandsänderung durch den Messprozess, Ann. Phys. (Leipzig) **8**, 322 (1951).